

On the Fractional Riemann-Liouville Integral of Gauss-Markov processes and applications

Mario Abundo*

Enrica Pirozzi †

Abstract

We investigate the stochastic processes obtained as the fractional Riemann-Liouville integral of order $\alpha \in (0, 1)$ of Gauss-Markov processes. The general expressions of the mean, variance and covariance functions are given. Due to the central rule, for the fractional integral of standard Brownian motion and of the non-stationary/stationary Ornstein-Uhlenbeck processes, the covariance functions are carried out in closed-form. In order to clarify how the fractional order parameter α affects these functions, their numerical evaluations are shown and compared also with those of the corresponding processes obtained by ordinary Riemann integral. The results are useful for fractional neuronal models with long range memory dynamics and involving correlated input processes. The simulation of these fractional integrated processes can be performed starting from the obtained covariance functions. A suitable neuronal model is proposed. Graphical comparisons are provided and discussed.

Keywords: Fractional integrals; Covariance function; Neuronal models; Simulation

Mathematics Subject Classification: 60G15, 26A33, 65C20.

1 Introduction

Although fractional calculus has the same ancient origins of the classical calculus, it has become of extreme interest in last decades for the researches, in many and different science fields. More recently, the theory and applications of fractional derivatives and fractional integrals ([36]) have been extensively developed by pure and applied mathematicians. Among a lot of motivations, we can claim that the researcher's community realized that fractional differential equations and related fractional integral solutions provide a natural framework for the description and the study of real phenomena such as, for instance, those occurring in biology, in ecology and in neuroscience (see, for instance, [9],[18],[25] and references therein).

Firstly, the integrals of stochastic processes constitute a mathematical subject fascinating especially probability theorists (see, for instance, [14], [39] and references therein); successively a wide audience was also attracted. Indeed, the need to describe complex phenomena, whose time evolution is affected by the history of own behavior ([16]) and by several memory effects of different nature ([20]), requires to design more elaborate mathematical models

*Dipartimento di Matematica, Università "Tor Vergata", via della Ricerca Scientifica, I-00133 Roma, Italy. E-mail: abundo@mat.uniroma2.it

†Dipartimento di Matematica e Applicazioni, Università "Federico II", via Cintia, complesso Monte S. Angelo, I-80126 Napoli, Italy. E-mail: enrica.pirozzi@unina.it

relying on integrals over time of stochastic processes, and some their modifications. Several aspects, particular cases and specific models can be found in [1]-[4]. In particular, in [4] we considered Gauss-Markov (GM) processes and their time integrals. Due to their easy mathematical handling, such kind of processes are suitable for modeling purposes, in a wide range of applications as, for instance, in computational neuroscience (see e.g. [44] and references therein), in finance mathematics (see e.g. [10]), in queueing theory and other applied sciences (see e.g. the discussion in [1], [2]). Moreover, as a specific example of application of integrated GM processes, we can refer to the context of neuronal modeling; indeed, some dynamics have been studied by introducing the so-called colored noise (i.e., a correlated GM process) in neuronal stochastic models, in place of the classical white noise (see e.g. [11], [22], [23], [32]). This kind of models rely on stochastic processes which are the integrals over time of an Ornstein-Uhlenbeck (OU) process, or more generally, of a GM process. Integrated GM processes and their first-passage times (FPT) were studied first in [1], [2], and then in [4].

With the aim to specialize this topic, in this paper we consider its extension to the fractional integration. Specifically, we investigate the stochastic processes obtained as Riemann-Liouville (RL) integral of GM processes. The motivation of this research is not only to shed light on such processes, investigating their properties, useful to consolidate their mathematical setting, but also to explore their powerful skills to model all phenomena that preserve their memory and are resultant of other dynamics evolving on different time-scales. The fractional integral reveals really suitable to specialize such kind of models; indeed, this mathematical tool plays the key rule for tuning the scale of the time, in such a way new features of the dynamical systems emerge and can be studied.

In the framework of neuronal dynamics, in [32], fractional stochastic models are introduced for preserving the memory of the neuronal membrane evolution; in such description, the parameter that affects the firing activity is the fractional order of the involved derivative. Simulation procedures are a first step in the investigation of such kind of models (see, for instance, [6],[32],[43]). The aim of giving a further contribution, that can be useful in the theoretical and simulation approaches to neuronal modeling, led us to consider this type of variable range memory process, obtained as the fractional integral over time of GM processes. An example of the mathematical extension of a classical model to the fractional one has been recently done, for instance, in a different context such as that of queueing systems in [7].

In this article, motivated by all above considerations, we study as replacing the ordinary Riemann integral with the fractional RL integral of order $\alpha \in (0, 1)$ affects the behavior, when α varies, of an integrated GM process. Due to their importance among GM processes, we mainly focus the attention on the fractional integral of the Brownian motion and OU processes. In particular, we consider the cases of stationary and non-stationary OU processes, because these two processes allow to design different neuronal models in which stimuli of different nature (exogenous and endogenous stimuli, respectively) can be included ([8]). A different approach has been considered in [38], where it was studied the power spectral density of RL fractional BM, in order to establish a fractional power law of the form $1/f^\alpha$; note that, for instance, this feature is observed in ordinary BM and its time integral. Moreover, in the present article, we do not even consider the fractional OU process as in [28], in which it is defined as the Riemann-Liouville of a tempered OU process (for some details on tempered fractional calculus see, e.g., [30] and references therein). Further investigations on such processes and comparisons with the processes here analyzed will be part of our future work.

Furthermore, as an example for possible applications, we consider the model for the neuronal activity based on the following coupled differential equations, for $t \geq 0$:

$$\mathcal{D}^\alpha V(t) = \frac{g_L}{C_m} V_L + \frac{\eta(t)}{C_m}, \quad V(0) = V_0 \quad (1.1)$$

$$d\eta(t) = -\frac{\eta(t) - I(t)}{\tau} dt + \frac{\xi}{\tau} dB(t), \quad \eta(0) = \eta_0. \quad (1.2)$$

In the (1.1) the derivative \mathcal{D}^α stands for the Caputo fractional derivative (specified in the next section); moreover, $\eta(t)$ is in place of the white noise $dB(t)$ as usual in the stochastic differential equation (SDE) of a Leaky Integrate-and-Fire (LIF) neuronal model (see, for example, [12]). The colored noise process $\eta(t)$ is the correlated process obeying to the SDE (1.2) and it is the input for the equation (1.1). The stochastic process $V(t)$ represents the voltage of the neuronal membrane, whereas the other parameters and functions are: C_m the membrane capacitance, g_L the leak conductance, V_L the resting (equilibrium) level potential, $I(t)$ the synaptic current (deterministic function), τ is the correlation time of $\eta(t)$ and $W(t)$ the noise (a standard Brownian motion). The initial values V_0 and η_0 can be specified constants or random variables, defining the above model as stationary or non-stationary one, respectively. $\eta(t)$ is a time-non-homogeneous GM process (OU-type). Finally, the solution process $V(t)$ of the equation (1.1) belongs to the class of the fractional RL integrals of the $\eta(t)$ GM process, that will be studied in this paper.

Note that, beyond the colored noise, the novelty of the above neuronal model, respect to the classical ones, is in the use of the fractional derivative in place of the integer one. The biophysical motivation is to describe a neuronal activity (by equation (1.1)) as a perfect integrator (without leakage) of the whole evolution of the input process $\eta(t)$ from an initial time until to the current time, but on a (more or less) finer time scale that can be regulated by choosing the fractional order of integration suitably adherent to the neuro-physiological evidences. Indeed, such a model can be useful, for instance, in the investigation and simulation of synchronous/asynchronous communications in networks of neurons ([42]).

We remark again that here we study the processes achieved applying the fractional RL integral to GM processes, and we investigate how the variation of the fractional order parameter affects the main features of these processes, such as mean, variance, covariance and paths. Furthermore, the mathematical results are shown, compared and discussed also in graphical way in figures carried out by numerical and simulation procedures. Finally, some indications about their usefulness for neuronal modelling are provided.

The paper is organized as follows. Section 2 contains mathematical formulation and details of the fractional RL integral of the BM (FIBM); plots of variance and covariance functions are provided by means of numerical evaluations; sample paths are also simulated for different values of α in order to show the qualitative behavior of the process. Our main result is in Section 3: the fractional RL integral of a GM process is defined and the covariance function is evaluated. Then, in Section 4, for the RL fractional integral of OU and stationary OU processes, the covariance functions are calculated and numerically evaluated carrying out comparisons between the fractional integral and the ordinary integral of these specific GM processes. Finally, in Section 5 we report some graphical comparisons and concluding remarks.

2 Mathematical formulation and preliminary results

At first, we start recalling some well-known definitions and introducing the object of our main interest.

Let be $\alpha \in (0, 1)$; if $f(t)$ is a real-valued differentiable function on \mathbb{R} , we recall that the *Caputo fractional derivative* of f of order α is defined by (see [13]):

$$\mathcal{D}^\alpha f(t) = \frac{1}{\Gamma(1-\alpha)} \int_0^t \frac{f'(s)}{(t-s)^\alpha} ds, \quad (2.1)$$

where f' denotes the ordinary derivative of f .

If f is a continuous function, its *fractional RL integral* of order α is defined by (see [15]):

$$\mathcal{J}^\alpha(f)(t) = \frac{1}{\Gamma(\alpha)} \int_0^t (t-s)^{\alpha-1} f(s) ds, \quad (2.2)$$

where Γ is the Gamma Euler function, i.e. $\Gamma(z) = \int_0^{+\infty} t^{z-1} e^{-t} dt$, $z > 0$. Notice that, taking the limit for $\alpha \rightarrow 1^-$, (2.1) provides the ordinary derivative of f , while (2.2) gives the ordinary Riemann integral of f ; moreover, by convention, $\mathcal{D}^0 f(t) = f(t) - f(0)$ and $\mathcal{J}^0(f)(t) = f(t)$ (for properties of Caputo fractional derivative and fractional RL integral, see e.g. [19],[27],[33],[36]).

Now, we recall the definition of GM process: let $m(t)$, $h_1(t)$, $h_2(t)$ be continuous functions of $t \geq 0$ which are C^1 in $(0, +\infty)$ and such that $h_2(t) \neq 0 \forall t \geq 0$, and let $r(t) = h_1(t)/h_2(t)$ be a non-negative, differentiable function, with $r'(t) > 0$ for $t > 0$, and $r(0) = r_0 \geq 0$. If, for $t \geq 0$, $B(t) = B_t$ denotes the standard Brownian motion (BM), such that $B(0) = 0$ with probability one (w.p.1), then

$$Y(t) = m(t) + h_2(t)B(r(t)), \quad t \geq 0, \quad (2.3)$$

is a continuous GM process with mean $m(t)$ and factorizable covariance $c(s, t) = h_1(s)h_2(t)$, for $0 \leq s \leq t$.

By substituting in (2.2) the function $f(t)$ with $Y(t)$ process, our aim is to study the fractional RL (pathwise) integral of the GM process $Y(t)$, namely the process

$$X^\alpha(t) = \mathcal{J}^\alpha(Y)(t) = \frac{1}{\Gamma(\alpha)} \int_0^t (t-s)^{\alpha-1} Y(s) ds. \quad (2.4)$$

Note that, due to the almost surely continuity of paths of the GM process $Y(t)$, the integral process $X^\alpha(t)$ is well defined and it is adapted in the same probability space of $Y(t)$.

Referring to the neuronal model (1.1)-(1.2), assuming that $V(0) = 0$ (and, in some cases, also $\eta(0) = 0$), the RL fractional integral \mathcal{J}^α is used as the left-inverse of the Caputo derivative \mathcal{D}^α (see, [21],[29]). In this way, we find that the solution $V(t)$ of (1.1)-(1.2) involves the RL fractional integral process of the GM process $\eta(t)$, i.e., specifically

$$\mathcal{J}^\alpha(\mathcal{D}^\alpha V(t)) = \mathcal{J}^\alpha \left(\frac{g_L}{C_m} V_L \right) + \mathcal{J}^\alpha \left(\frac{\eta(t)}{C_m} \right), \quad \text{with } V(0) = 0. \quad (2.5)$$

The investigation of the last term in the right-hand-side of the above equation has to be done. We proceed in this direction in the following.

2.1 The fractional Riemann-Liouville integral of BM (FIBM)

As a first case, we consider the icon of the non-stationary GM processes: the standard Brownian motion. Let us consider the fractional Riemann-Liouville integral of B_t (FIBM), that is

$$\mathcal{J}^\alpha(B)(t) = \frac{1}{\Gamma(\alpha)} \int_0^t (t-s)^{\alpha-1} B(s) ds.$$

It has not an immediate application in the neuronal model (1.1)-(1.2), but it will play a role in the construction of fractional integrals of GM processes. Nevertheless, a possible model that can be suitable designed is that composed by the following coupled equations:

$$\mathcal{D}^\alpha V(t) = \frac{g_L}{C_m} V_L + \frac{\eta(t)}{C_m}, \quad V(0) = 0, \quad (2.6)$$

$$d\eta(t) = \frac{\zeta}{\tau} dB(t), \quad \eta(0) = 0, \quad (2.7)$$

that, for $V_L = 0, C_m = 1$, are solved by the fractional integral process of a Brownian motion $B(t)$, i.e.

$$\mathcal{J}^\alpha(\mathcal{D}^\alpha V) = \mathcal{J}^\alpha(\eta) = \frac{\zeta}{\tau} \mathcal{J}^\alpha(B).$$

Note that the SDE (2.7) is a prototype of integrate-and-fire neuronal models ([26]). The above model describes the neuronal membrane voltage as the fractional integral of a Brownian input process. About such kind of processes, the following holds.

Proposition 2.1 *For $0 \leq \alpha \leq 1$, let be $\mathcal{J}^\alpha(B)(t)$ the fractional RL integral of B_t of order α ; then, for $0 \leq u \leq t$, the covariance of $\mathcal{J}^\alpha(B)(u)$ and $\mathcal{J}^\alpha(B)(t)$ is:*

$$\text{cov}(\mathcal{J}^\alpha(B)(u), \mathcal{J}^\alpha(B)(t)) = \frac{1}{\Gamma^2(\alpha)} \left[\frac{t^{\alpha+1} u^\alpha}{\alpha^2(\alpha+1)} - \frac{tH_\alpha(u, t)}{\alpha(\alpha+1)} + \frac{J_\alpha(u, t)}{\alpha(\alpha+1)} \right] \quad (2.8)$$

where

$$J_\alpha(u, t) = \int_0^u s(u-s)^{\alpha-1} (t-s)^\alpha ds, \quad (2.9)$$

$$H_\alpha(u, t) = \int_0^u (u-s)^{\alpha-1} (t-s)^\alpha ds. \quad (2.10)$$

Taking $u = t$ in (2.8), one gets the variance of $\mathcal{J}^\alpha(B)(t)$:

$$\text{Var}(\mathcal{J}^\alpha(B)(t)) = \frac{1}{\Gamma^2(\alpha)} \cdot \frac{t^{2\alpha+1}}{\alpha^2(2\alpha+1)} = \frac{t^{2\alpha+1}}{(2\alpha+1)\Gamma^2(\alpha+1)}. \quad (2.11)$$

Proof. Since $E(B(s)B(v)) = \min(s, v)$, we have for $u \leq t$:

$$\begin{aligned} \text{cov}(\mathcal{J}^\alpha(B)(u), \mathcal{J}^\alpha(B)(t)) &= \frac{1}{\Gamma^2(\alpha)} E \left(\int_0^u (u-s)^{\alpha-1} B(s) ds \cdot \int_0^t (t-v)^{\alpha-1} B(v) dv \right) \\ &= \frac{1}{\Gamma^2(\alpha)} \int_0^u ds \int_0^t dv (u-s)^{\alpha-1} (t-v)^{\alpha-1} \min(s, v); \end{aligned} \quad (2.12)$$

the last integral can be split into three parts:

$$\begin{aligned} & \int_0^u ds \int_0^s dv (u-s)^{\alpha-1} (t-v)^{\alpha-1} v + \int_0^u ds \int_s^u dv (u-s)^{\alpha-1} (t-v)^{\alpha-1} s \\ & \quad + \int_0^u ds \int_u^t dv (u-s)^{\alpha-1} (t-v)^{\alpha-1} s = I_1 + I_2 + I_3, \end{aligned} \quad (2.13)$$

where, for simplicity of notations we let drop the dependence of I_i on α .

We have:

$$I_1 = \int_0^u (u-s)^{\alpha-1} ds \int_0^s (t-v)^{\alpha-1} v dv;$$

the inner integral is equal to

$$\frac{(t-s)^{\alpha+1}}{\alpha+1} - \frac{t(t-s)^\alpha}{\alpha} + \frac{t^{\alpha+1}}{\alpha(\alpha+1)}.$$

Then, by straightforward calculation, we obtain

$$\begin{aligned} I_1 &= \frac{t^{\alpha+1} u^\alpha}{\alpha^2(\alpha+1)} - \frac{t}{\alpha(\alpha+1)} \int_0^u (u-s)^{\alpha-1} (t-s)^\alpha ds - \frac{1}{\alpha+1} \int_0^u s (u-s)^{\alpha-1} (t-s)^\alpha ds \\ &= \frac{t^{\alpha+1} u^\alpha}{\alpha^2(\alpha+1)} - \frac{t}{\alpha(\alpha+1)} H_\alpha(u, t) - \frac{1}{\alpha+1} J_\alpha(u, t), \end{aligned}$$

where $J_\alpha(u, t)$ and $H_\alpha(u, t)$ are given by (2.9) and (2.10). As for the second integral, we have:

$$\begin{aligned} I_2 &= \frac{1}{\alpha} \left[\int_0^u s (u-s)^{\alpha-1} (t-s)^\alpha ds - (t-u)^\alpha \int_0^u s (u-s)^{\alpha-1} ds \right] \\ &= \frac{1}{\alpha} J_\alpha(u, t) - \frac{1}{\alpha} (t-u)^\alpha \frac{u^{\alpha+1}}{\alpha(\alpha+1)}. \end{aligned}$$

The third integral is:

$$I_3 = \left(\int_0^u s (u-s)^{\alpha-1} ds \right) \left(\int_u^t (t-v)^{\alpha-1} dv \right) = \frac{u^{\alpha+1}}{\alpha^2(\alpha+1)} \cdot (t-u)^\alpha.$$

Finally, by summing the three integrals, and inserting in (2.13), we obtain (2.8).

To obtain the variance, it is enough to put $u = t$ in (2.8) and to note that $J_\alpha(t, t) = \frac{t^{2\alpha+1}}{2\alpha(2\alpha+1)}$ and $H_\alpha(t, t) = \frac{t^{2\alpha}}{2\alpha}$; then, (2.11) follows. \square

Remark 2.2 For $\alpha = 1$ one has $J_1(u, t) = tu^2/2 - u^3/3$ and $H_1(u, t) = t^2/2 - (t-u)^2/2$, so from (2.8) one gets the well-known covariance function of integrated BM (see e.g [35]):

$$\text{cov} \left(\int_0^u B_s ds, \int_0^t B_v dv \right) = u^2 \left(\frac{t}{2} - \frac{u}{6} \right); \quad (2.14)$$

moreover, from (2.11), its variance follows:

$$\text{var} \left(\int_0^t B_s ds \right) = t^3/3. \quad (2.15)$$

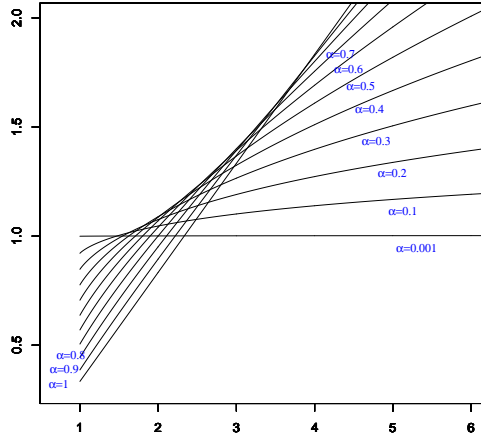


Figure 1: Plot of the covariance function of FIBM, $cov(\mathcal{J}^\alpha(B)(u), \mathcal{J}^\alpha(B)(t))$, given by (2.8), as a function of $t \geq u$, for $u = 1$ fixed, and various values of $\alpha \in (0, 1)$. The horizontal line represents the covariance calculated for $\alpha = 0$; the curve corresponding to $\alpha = 1$ matches the straight line of equation $y = t/2 - 1/6$.

2.1.1 Numerical evaluations: the FIBM covariance

We have computed $cov(\mathcal{J}^\alpha(B)(u), \mathcal{J}^\alpha(B)(t))$ for various values of α and $u \leq t$; since $J_\alpha(u, t)$ and $H_\alpha(u, t)$ cannot be obtained in closed form for any α , their value has been obtained by numerical integration.

In the Figure 1, we report the graph of $cov(\mathcal{J}^\alpha(B)(u), \mathcal{J}^\alpha(B)(t))$ given by (2.8), as a function of $t \geq u$, for $u = 1$ fixed, and various values of $\alpha \in (0, 1)$.

In the Figures 2 we report the graph of the same covariance as a function of $\alpha \in (0, 1)$, for $u = 1$ and various values of $t \geq 1$.

It appears that, for fixed u and α the covariance function of $\mathcal{J}^\alpha(B)(t)$ increases, as a function of $t \geq u$. For fixed u , there exists a value \bar{t}_u such that for $t < \bar{t}_u$ the covariance function is decreasing as a function of α , while for $t > \bar{t}_u$ it is increasing (for $u = 1$ one has $\bar{t}_u \simeq 1.5$, see Figure 1).

Moreover, for fixed u and t , a value $\bar{\alpha}_t$ exists at which the covariance attains its maximum, that is, for $\alpha \leq \bar{\alpha}_t$ the covariance function is increasing, as a function of α , while it is decreasing for $\alpha > \bar{\alpha}_t$ (see Figure 2).

Of course, since $\mathcal{J}^0(B)(t) = B(t)$, for $1 = u \leq t$ one has

$$cov(\mathcal{J}^0(B)(u), \mathcal{J}^0(B)(t)) = cov(B(u), B(t)) = \min(u, t) = 1.$$

Notice that the value $\alpha = 0$ cannot be directly substituted in (2.8), because $J_\alpha(u, t)$, $H_\alpha(u, t)$ and $\Gamma(\alpha)$ diverge, as $\alpha \rightarrow 0^+$. Thus, numerical calculation allows only to evaluate the covariance for small, but positive α (in fact, we have taken $\alpha = 0.001$).

For $\alpha = 1$, we recover the covariance of integrated BM; in fact, for $u = 1$ it is equal to $t/2 - 1/6$ (see (2.14)) whose graph matches the curve obtained for $\alpha = 1$.

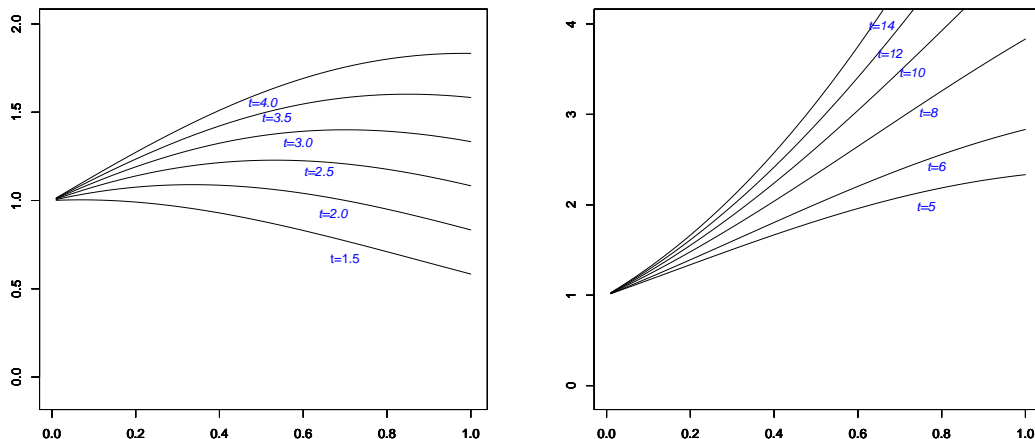


Figure 2: Plot of the covariance function of FIBM, given by (2.8), as a function of $\alpha \in (0, 1)$, for $u = 1$ and $t = 1.5, 2, 2.5, 3, 3.5, 4$ (left panel); $t = 5, 6, 8, 10, 12, 14$ (right panel). The larger t , the higher the curve.

3 The fractional Riemann-Liouville integral of a Gauss-Markov process

Let us consider the GM process $Y(t)$ given by (2.3); we have

$$\begin{aligned} \mathcal{J}^\alpha(Y)(t) &= \frac{1}{\Gamma(\alpha)} \int_0^t (t-s)^{\alpha-1} Y(s) ds = \frac{1}{\Gamma(\alpha)} \int_0^t (t-s)^{\alpha-1} [m(s) + h_2(s)B(r(s))] ds \\ &= \frac{1}{\Gamma(\alpha)} \int_0^t [\tilde{m}(s, t) + \tilde{h}_2(s, t)B(r(s))] ds, \end{aligned} \quad (3.1)$$

where

$$\tilde{m}(s, t) = (t-s)^{\alpha-1} m(s), \quad \tilde{h}_2(s, t) = (t-s)^{\alpha-1} h_2(s) \quad (3.2)$$

(here, the dependence on α was omitted to avoid an heavy notation). Then, by straightforward calculations, and applying the linearity in L^1 of the fractional RL integral operator, we obtain:

Proposition 3.1 *The fractional RL integral of $Y(t)$,*

$$\mathcal{J}^\alpha(Y)(t) = \frac{1}{\Gamma(\alpha)} \int_0^t (t-s)^{\alpha-1} Y(s) ds, \quad (3.3)$$

is normally distributed with mean $M(t) = \frac{1}{\Gamma(\alpha)} \int_0^t \tilde{m}(s, t) ds$ and covariance, for $0 \leq u \leq t$:

$$\begin{aligned} \text{cov}(\mathcal{J}^\alpha(Y)(u), \mathcal{J}^\alpha(Y)(t)) &= \frac{1}{\Gamma^2(\alpha)} \text{cov} \left(\int_0^u \tilde{h}_2(s, t) B(r(s)) ds, \int_0^t \tilde{h}_2(v, t) B(r(v)) dv \right) \\ &= \frac{1}{\Gamma^2(\alpha)} \int_0^u ds \int_0^t dv \tilde{h}_2(s, t) \tilde{h}_2(v, t) \min(r(s), r(v)). \end{aligned} \quad (3.4)$$

Remark 3.2 *The integral in (3.4) can be calculated, by splitting it into three parts, as in the proof of Proposition 2.1; thus, one obtains:*

$$\begin{aligned} \text{cov}(\mathcal{J}^\alpha(Y)(u), \mathcal{J}^\alpha(Y)(t)) &= \frac{1}{\Gamma^2(\alpha)} \left[\int_0^u ds (u-s)^{\alpha-1} h_2(s) \int_0^s dv (t-v)^{\alpha-1} r(v) h_2(v) \right. \\ &\quad \left. + \int_0^u ds (u-s)^{\alpha-1} h_2(s) r(s) \int_s^u dv (t-v)^{\alpha-1} h_2(v) \right. \\ &\quad \left. + \left(\int_0^u ds (u-s)^{\alpha-1} r(s) h_2(s) \right) \left(\int_u^t dv (t-v)^{\alpha-1} h_2(v) \right) \right] := \frac{1}{\Gamma^2(\alpha)} [\tilde{I}_1 + \tilde{I}_2 + \tilde{I}_3], \end{aligned} \quad (3.5)$$

where, for simplicity of notations we let drop the dependence of \tilde{I}_i on α . For $u = t$, \tilde{I}_3 vanishes and $\tilde{I}_2 = \tilde{I}_1$, so one has:

$$\text{Var}(\mathcal{J}^\alpha(Y)(t)) = \frac{2}{\Gamma^2(\alpha)} \int_0^t ds (t-s)^{\alpha-1} h_2(s) \int_0^s dv (t-v)^{\alpha-1} r(v) h_2(v). \quad (3.6)$$

4 Fractional integral of GM processes and comparisons with the ordinary integral of GM processes

In this section, we study the qualitative behavior of the fractional integral over time of a GM process, when varying the order $\alpha \in (0, 1)$, and we compare it with the corresponding ordinary integral. Computer simulation is also used to illustrate these behaviors. First, we recall from [4] the following result, regarding the ordinary integral over time of a GM process.

Theorem 4.1 *Let Y be a GM process of the form (2.3) with $r(0) = r_0 \geq 0$, $r'(t) > 0$ for $t > 0$; then $X(t) = x + \int_0^t Y(s) ds$ can be written as $\mathcal{V}(t) + \eta \int_0^t h_2(s) ds$, in which $\eta = B(r(0))$ and $\mathcal{V}(t)$ is normally distributed with mean $x + M(t)$ and variance $\gamma(\rho(t))$, where $\rho(t) = r(t) - r(0)$, $M(t) = \int_0^t m(s) ds$, $\gamma(t) = \int_0^t (R(t) - R(s))^2 ds$ and $R(t) = \int_0^t h_2(\rho^{-1}(s)) / \rho'(\rho^{-1}(s)) ds$.*

□

Note that, generally the $\mathcal{V}(t)$ process and the r.v. η are not independent, when $r(0) \neq 0$ (if $r(0) = 0$, then the term η vanishes).

4.1 Fractional integrated BM (FIBM)

If $Y(t) = B_t$, taking $m(t) = 0$, $h_2(t) = 1$, $r(t) = \rho(t) = t$ in Theorem 4.1, we have for the ordinary integral of BM:

$$\int_0^t B_s ds \sim \mathcal{N}(0, t^3/3), \quad (4.1)$$

where $\mathcal{N}(\mu, \sigma^2)$ denotes a Gaussian r.v. with mean μ and variance σ^2 .

By using Proposition 2.1, we obtain that the fractional integral of order α , i.e.

$$\mathcal{J}^\alpha(B)(t) = \frac{1}{\Gamma(\alpha)} \int_0^t (t-s)^{\alpha-1} B_s ds \sim \mathcal{N}(0, t^{2\alpha+1} / [\alpha^2(2\alpha+1)\Gamma^2(\alpha)]).$$

Thus, we have:

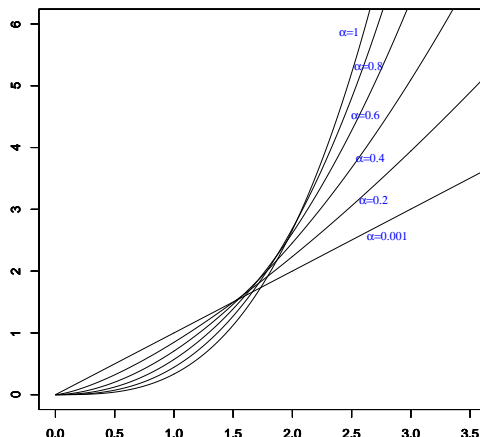


Figure 3: Plot of the variance of FIBM, $\mathcal{J}^\alpha(B)(t)$, given by (2.11), as a function of $t \in [0, 3.5]$, for various values of $\alpha \in (0, 1)$. The time zone at which an inversion of behavior is observed goes from $t \simeq 1.73$ to $t \simeq 1.77$. For $\alpha = 0.001$ the curve is close to the graph of the function $v(t) = t$, since for $\alpha = 0$ FIBM becomes BM; for $\alpha = 1$ the curve matches the graph of the function $v(t) = t^3/3$, since FIBM becomes the ordinary integral of BM.

- for $\alpha \rightarrow 0^+$, $\mathcal{J}^\alpha(B)(t) \sim \mathcal{N}(0, t)$, because $\alpha\Gamma(\alpha) = \Gamma(\alpha + 1)$ and so $\alpha^2(2\alpha + 1)\Gamma^2(\alpha)$ tends to $\Gamma^2(1) = 1$; therefore, $\mathcal{J}^0(B)(t)$ has the same distribution as B_t .
- for $\alpha = 1/2$, one has $\mathcal{J}^\alpha(B)(t) \sim \mathcal{N}(0, 2t^2/\pi)$, because $\Gamma(1/2) = \sqrt{\pi}$.
- for $\alpha \rightarrow 1^-$, one has $\mathcal{J}^\alpha(B)(t) \sim \mathcal{N}(0, t^3/3)$, because the fractional integral coincides with the ordinary integral.

4.1.1 Numerical evaluations of the FIBM variance and simulation paths

In the Figure 3 we report the shape of the variance of $\mathcal{J}^\alpha(B)(t)$, i.e. $t^{2\alpha+1}/[(2\alpha+1)\Gamma^2(\alpha+1)]$, as a function of $t > 0$, for various values of $\alpha \in (0, 1)$. As we see, for fixed α the variance is increasing, as a function of t . Moreover, for small enough values of t , the curves become ever lower, as α increases, that is, the variance decreases as a function of α ; for larger enough values of t this behavior is overturned, because the variance increases with α . The time zone at which an inversion of behavior is observed goes from $t \simeq 1.73$ to $t \simeq 1.77$. For $\alpha = 0.001$ the curve is close to the graph of the function $v(t) = t$, since for $\alpha = 0$ FIBM becomes BM; for $\alpha = 1$ the curve matches the graph of the function $v(t) = t^3/3$, since FIBM becomes the ordinary integral of BM.

In the Figure 4 we report the graphs of simulated trajectories of FIBM as function of time t , for some values of $\alpha \in (0, 1)$.

Specifically, the sample paths have been obtained by using the **R** software, with time discretization step $h = 0.01$ and by means of the same sequence of pseudo-random Gaussian numbers. Our simulation algorithm has been realized as an R script. Referring to algorithms for the generation of pseudo-random numbers (see, for instance, [17]), the main steps of implementation are the following:

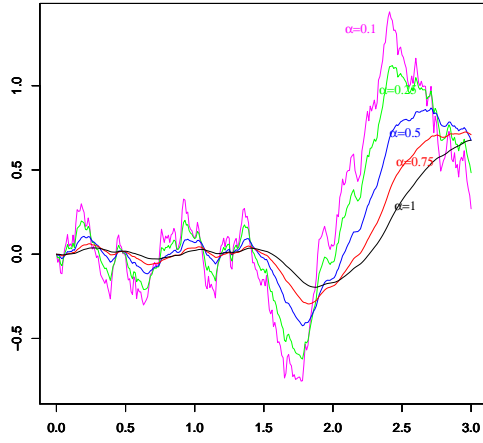


Figure 4: Simulated trajectories of FIBM as function of time t , for some values of $\alpha \in (0, 1)$.

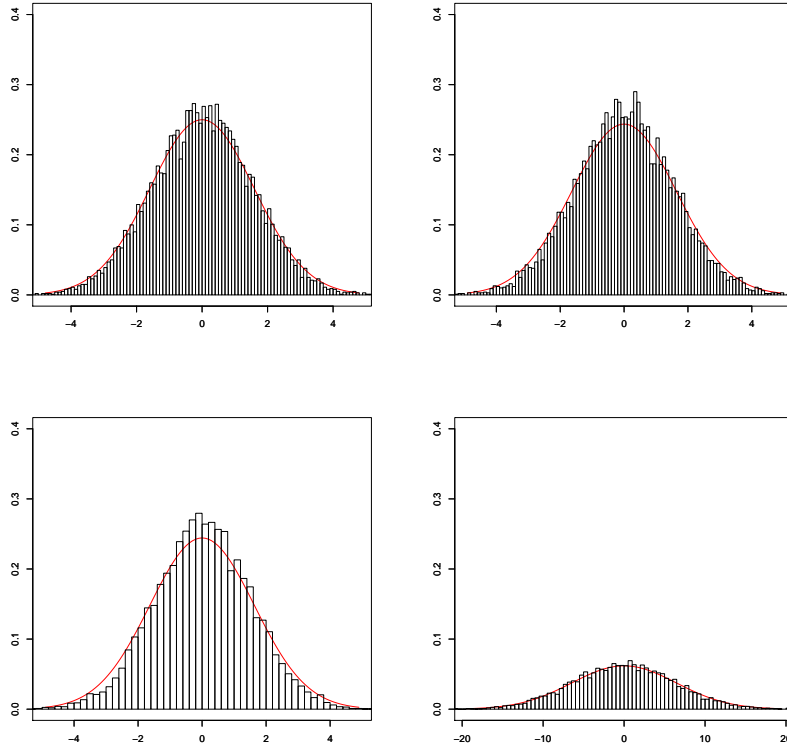


Figure 5: On top: Comparison between the density histogram of simulated values of FIBM at $t = 2$, and the Gaussian density with zero mean and variance given by (2.11), for $\alpha = 0.5$ (left) and $\alpha = 0.75$ (right). On Bottom: Comparison between the density histogram of simulated values of FIBM with $\alpha = 1$, at $t = 2$, and the Gaussian density with zero mean and variance given by (2.11), (left); the same for $\alpha = 1$ and $t = 5$ (right).

- calculation of the elements of $N \times N$ covariance matrix $C(t_i, t_j)$ at times $t_i, i = 1, \dots, N$, of an equi-spaced temporal grid;
- application of the Cholesky decomposition algorithm to the covariance matrix C to obtain a lower triangular matrix $L(i, j)$ such that $C = LL^T$;
- generation of a N -dimensional array \mathbf{z} of standard pseudo-Gaussian numbers;
- construction of the sequence of simulated values of the correlated fractional integrated process as the array $\mathbf{x} = L\mathbf{z}$.

Finally, the array \mathbf{x} provides the simulated path $(X(t_1), \dots, X(t_N))$, which components have the assigned covariance.

In particular, in the Figure 5, we compare the density histogram of simulated values of FIBM at a certain time t , with the Gaussian density with zero mean and variance given by (2.11), for various values of α . As we see, the matching is very good.

4.2 Fractional integrated OU (FIOU) process

Let be $Y_{OU}(t)$ the (non stationary) OU process, given by the solution of the SDE:

$$dY_{OU}(t) = -\mu(Y_{OU}(t) - \beta)dt + \sigma dB_t, \quad Y_{OU}(0) = y, \quad (4.2)$$

where $\mu, \sigma > 0$ and $\beta \in (-\infty, +\infty)$. The explicit solution is (see e.g. [5]):

$$Y_{OU}(t) = \beta + e^{-\mu t}[y - \beta + \tilde{B}(\rho(t))], \quad (4.3)$$

where $\tilde{B}(t)$ is standard BM and

$$r(t) = \rho(t) = \frac{\sigma^2}{2\mu} (e^{2\mu t} - 1) \quad (4.4)$$

(notice that $r(0) = 0$). So, $Y_{OU}(t)$ is a GM process with:

$$m(t) = \beta + e^{-\mu t}(y - \beta), \quad (4.5)$$

$$h_1(t) = \frac{\sigma^2}{2\mu} (e^{\mu t} - e^{-\mu t}), \quad h_2(t) = e^{-\mu t} \quad (4.6)$$

and covariance

$$c(s, t) = h_1(s)h_2(t) = \frac{\sigma^2}{2\mu} (e^{-\mu(t-s)} - e^{-\mu(s+t)}), \quad 0 \leq s \leq t. \quad (4.7)$$

Referring to the neuronal model, i.e. to the equations (1.1)-(1.2), the OU process $Y_{OU}(t)$ stands for the process $\eta(t)$ solution of (1.2) if one takes $\tau = 1/\mu$, $\varsigma/\tau = \sigma$ and a constant input current β in place of the $I(t)$.

By calculating the various quantities in Theorem 4.1, we get (see [2]):

$$M(t) = \int_0^t (\beta + e^{-\mu s}(x - \beta)) ds = \beta t + \frac{(x - \beta)}{\mu} (1 - e^{-\mu t}), \quad (4.8)$$

$$\rho^{-1}(s) = \frac{1}{2\mu} \ln \left(1 + \frac{2\mu}{\sigma^2} s \right), \quad R(t) = \int_0^t e^{-\mu\rho^{-1}(s)} (\rho^{-1})'(s) ds = \frac{1 - e^{-\mu\rho^{-1}(t)}}{\mu}, \quad (4.9)$$

$$\begin{aligned} \gamma(t) &= \frac{1}{\mu^2} \int_0^t \left(e^{-\mu\rho^{-1}(t)} - e^{-\mu\rho^{-1}(s)} \right)^2 ds = \frac{1}{\mu^2} \int_0^t \left(\frac{1}{\sqrt{1 + 2\mu t/\sigma^2}} - \frac{1}{\sqrt{1 + 2\mu s/\sigma^2}} \right)^2 ds \\ &= \frac{\sigma^2 t}{\mu^2(\sigma^2 + 2\mu t)} - \frac{2\sigma^2}{\mu^3 \sqrt{1 + 2\mu t/\sigma^2}} \left(\sqrt{1 + 2\mu t/\sigma^2} - 1 \right) + \frac{\sigma^2}{2\mu^3} \ln(1 + 2\mu t/\sigma^2). \end{aligned} \quad (4.10)$$

Thus, by Theorem 4.1, being $\eta = B(r(0)) = B(0) = 0$, we obtain that the integrated OU (IOU) process (i.e. the ordinary integral over time of the OU process)

$$X_{IOU}(t) = \int_0^t Y_{OU}(s) ds = \mathcal{J}^1(Y_{OU})(t) \quad (4.11)$$

is normally distributed with mean $M(t)$ and variance $\gamma(\rho(t))$. By calculation, one obtains:

$$\text{var}(X_{IOU}(t)) = \frac{\sigma^2}{2\mu^3} [1 - e^{-2\mu t} - 4(1 - e^{-\mu t}) + 2\mu t], \quad t \geq 0. \quad (4.12)$$

As far as the FIOU, i.e. $\mathcal{J}^\alpha(Y_{OU})(t)$, is concerned, by Proposition 3.1 we get that it has normal distribution with mean $M(t) = \frac{1}{\Gamma(\alpha)} \int_0^t \tilde{m}(s, t) ds$, and covariance and variance respectively given by (3.5) and (3.6), where $r(t)$ is as in (4.4), \tilde{m} , \tilde{h}_2 are the corresponding functions obtained inserting (4.5), (4.6) in (3.2). Precisely, the integrals in (3.5) turn out to be:

$$\begin{aligned} \tilde{I}_1 &= \frac{\sigma^2}{\mu} \int_0^u ds (u-s)^{\alpha-1} e^{-\mu s} \int_0^s dv (t-v)^{\alpha-1} \sinh(\mu v), \\ \tilde{I}_2 &= \frac{\sigma^2}{\mu} \int_0^u ds (u-s)^{\alpha-1} \sinh(\mu s) \int_s^u dv (t-v)^{\alpha-1} e^{-\mu v}, \\ \tilde{I}_3 &= \frac{\sigma^2}{\mu} \left(\int_0^u ds (u-s)^{\alpha-1} \sinh(\mu s) \right) \left(\int_u^t dv (t-v)^{\alpha-1} e^{-\mu v} \right). \end{aligned} \quad (4.13)$$

Notice that, for $\sigma = 1$ and $\mu \rightarrow 0$ one obtains again the integrals I_i , $i = 1, 2, 3$ in (2.13), since $Y_{OU}(t)$ approaches BM.

Taking $\alpha = 1$ in the expressions above, by (3.5) one obtains the covariance of the ordinary integral of OU (IOU):

$$\begin{aligned} &\text{cov}(\mathcal{J}^1(Y_{OU})(u), \mathcal{J}^1(Y_{OU})(t)) \\ &= \frac{\sigma^2}{2\mu^3} (2\mu u + 4e^{-\mu u} - e^{-\mu(t-u)} - e^{-\mu(t+u)} + 2e^{-\mu t} - 2e^{-\mu u} - 2), \quad 0 \leq u \leq t. \end{aligned} \quad (4.14)$$

4.2.1 Numerical evaluations: The FIOU variance and covariance

As we see, for α different from 0 and 1, the calculations required to find the covariance of FIOU are far more complicated than in the case of FIBM; in fact, \tilde{I}_i are double integrals which cannot be found analytically, so we have calculated them numerically, by using the **R** software.

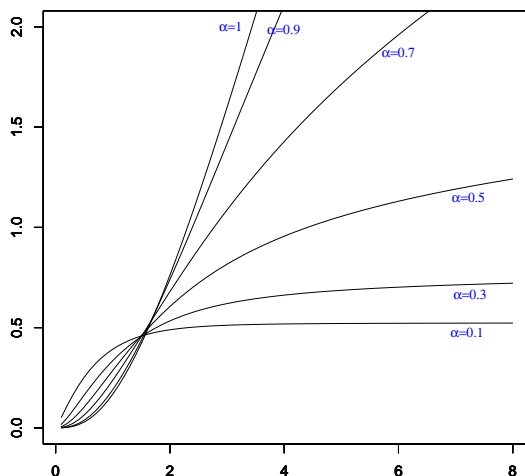


Figure 6: Plot of the variance of FIOU, $\mathcal{J}^\alpha(Y_{OU})(t)$ with $\sigma = \mu = 1$, as a function of $t \in [0, 8]$, for various values of $\alpha \in (0, 1)$. The time zone at which an inversion of behavior is observed goes from $t \simeq 1.73$ to $t \simeq 1.77$. For $\alpha = 0.1$ the curve is close to the graph of the function $Var(t) = \frac{\sigma^2}{2\mu}(1 - \exp(-2\mu t))$ (i.e. the variance of OU); for $\alpha = 1$ the curve matches the graph of the function $\gamma(\rho(t))$ (i.e. the variance of IOU), given by (4.12), since FIOU becomes the ordinary integral of OU.

With reference to OU process with $\sigma = \mu = 1$, in the Figure 6, for $u = 1$ and $u \leq t \leq 2$, and several values of α , we report the shape of the variance of $\mathcal{J}^\alpha(Y_{OU})(t)$. As we see, for fixed α the variance is increasing, as a function of t . Moreover, for small enough values of t , the curves become ever lower, as α increases, that is, the variance decreases as a function of α ; for larger enough values of t this behavior is overturned, because the variance increases with α . In fact, it appears a behavior analogous to that of the variance of the FIBM (see Figure 3); the time zone at which an inversion of behavior is detected, is the same observed for the variance of the FIBM. For $\alpha = 0.1$ the curve is close to the graph of the function $v(t) = \frac{\sigma^2}{2\mu}(1 - \exp(-2\mu t))$ (i.e. the variance of OU); for $\alpha = 1$ the curve matches the graph of the function $\gamma(\rho(t))$ (i.e. the variance of IOU), given by (4.12), since FIOU becomes the ordinary integral of OU.

In the Figure 7 the $cov(\mathcal{J}^\alpha(Y_{OU})(u), \mathcal{J}^\alpha(Y_{OU})(t))$, for $u = 1$ and $u \leq t \leq 2$, for various values of α . We note that for $\alpha = 0.01$ the curve is close to the covariance of OU, given by (4.7) (red curve), for $\alpha = 0.99$ the curve is close to that of the covariance of the ordinary integral of OU (IOU), given by (4.14) (green curve).

In the Figures 11 and 12 of the last section, for further comparisons between the considered processes, we report the three-dimensional plot and two-dimensional color plot, respectively, of the covariance function of FIOU, $c(u, t) = cov(\mathcal{J}^\alpha(Y_{OU})(u), \mathcal{J}^\alpha(Y_{OU})(t))$, for various values of α . These illustrate globally the behavior of the covariance function of FIOU, for any u and t ; note, for instance, that for $u = t$ they match the behavior shown in the Figure 6.

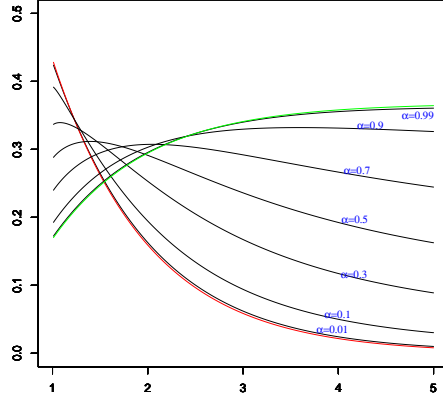


Figure 7: Plot of the covariance of FIOU, $cov(\mathcal{J}^\alpha(Y_{OU})(u), \mathcal{J}^\alpha(Y_{OU})(t))$, with $\sigma = \mu = 1$, for $1 = u \leq t \leq 5$, and various values of $\alpha \in (0, 1)$. For $\alpha = 0.01$ the curve is close to the covariance of OU, given by (4.7) (red curve), for $\alpha = 0.99$ the curve is close to that of the covariance of the ordinary integral of OU (IOU), given by (4.14) (green curve).

4.3 Fractional integrated stationary OU (FISOU) process

For $\mu > 0$ and $\sigma \neq 0$, the *stationary OU* (SOU) process is defined by

$$Y_{SOU}(t) = e^{-\mu t} B \left(\frac{\sigma^2}{2\mu} e^{2\mu t} \right); \quad (4.15)$$

therefore, the SOU process is a GM process with

$$r(t) = \frac{\sigma^2}{2\mu} e^{2\mu t}, \quad m(t) = 0, \quad (4.16)$$

$$h_1(t) = \frac{\sigma^2}{2\mu} e^{\mu t}, \quad h_2(t) = e^{-\mu t}, \quad (4.17)$$

and covariance

$$c(s, t) = \frac{\sigma^2}{2\mu} e^{-\mu(t-s)}, \quad s \leq t. \quad (4.18)$$

One has $var(Y_{SOU}(t)) = \frac{\sigma^2}{2\mu}$ and $Y_{SOU}(t)$ admits a steady-state distribution, which is $\mathcal{N}(0, \sigma^2/2\mu)$. Moreover, $r(0) = \frac{\sigma^2}{2\mu} > 0$, $\eta = B(\frac{\sigma^2}{2\mu})$, $\rho(t) = r(t) - r(0) = \frac{\sigma^2}{2\mu} (e^{2\mu t} - 1)$, $h_1(t)$ and $h_2(t)$ are the same functions of (non stationary) OU.

Referring to the neuronal model (1.1)-(1.2), the $\eta(t)$ process solving the equation (1.2), with η_0 r.v., is a stationary OU process as above specified. A specific example of application can be found in [37]. It is usually used for modeling correlated exogenous inputs.

Then, by Theorem 4.1 the integrated SOU (ISOU) process (i.e. the ordinary integral over time of the SOU process) is:

$$X_{ISOU}(t) = \int_0^t Y_{SOU}(s) ds = \int_0^t e^{-\mu s} B(\rho(s)) ds + \eta \int_0^t e^{-\mu s} ds \quad (4.19)$$

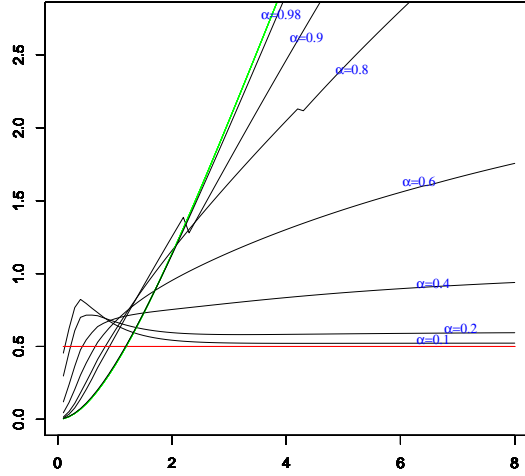


Figure 8: Plot of the variance of FISOU, $J^\alpha(Y_{SOU})(t)$ with $\sigma = \mu = 1$, as a function of $t \in [0, 8]$, for various values of $\alpha \in (0, 1)$. The time zone at which an inversion of behavior is observed goes from $t \simeq 1.7$ to $t \simeq 1.8$. For $\alpha = 0.1$ the curve is close to the graph of the function $v(t) = \sigma^2/2\mu$ (i.e. the variance of SOU, red), since FISOU for $\alpha = 0$ becomes SOU; for $\alpha \approx 1$ the curve matches the graph of the function $v(t) = \frac{\sigma^2}{\mu^3}(\mu t + e^{-\mu t} - 1)$ (i.e. the variance of ISOU, green), given by (4.22), since FISOU becomes the ordinary integral of SOU.

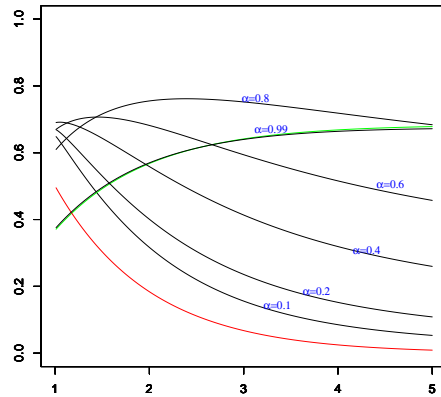


Figure 9: Plot of the covariance of FISOU, $cov(J^\alpha(Y_{SOU})(u), J^\alpha(Y_{SOU})(t))$, with $\sigma = \mu = 1$, for $1 = u \leq t \leq 5$, and various values of $\alpha \in (0, 1)$. For $\alpha = 0.0$, the red curve is the covariance of SOU, given by (4.18), for $\alpha = 1$ the green curve is the covariance of the ordinary integral of SOU (ISOU), given by (4.21).

$$= \int_0^{\rho(t)} \frac{e^{-\mu\rho^{-1}(u)}}{\rho'(\rho^{-1}(u))} B(u) du + \left(\frac{1 - e^{-\mu t}}{\mu} \right) \eta. \quad (4.20)$$

Thus, for fixed t , $X_{ISOU}(t)$ turns out to be the sum of two (correlated) Gaussian r.v. W_1 and W_2 with zero mean; the variance of W_1 can be calculated by Theorem 4.1, while $var(W_2) = \sigma^2 \frac{(1 - e^{-\mu t})^2}{2\mu^3}$. The covariance function of ISOU $X_{ISOU}(t)$ was calculated in [4]; it holds (see also [41]):

$$cov(X_{ISOU}(t), X_{ISOU}(s)) = \frac{\sigma^2}{2\mu^3} (2\mu \min(s, t) + e^{-\mu s} + e^{-\mu t} - e^{-\mu|t-s|} - 1), \quad (4.21)$$

and so

$$var(X_{ISOU}(t)) = \frac{\sigma^2}{\mu^3} (\mu t + e^{-\mu t} - 1). \quad (4.22)$$

As far as the fractional integral $\mathcal{J}^\alpha(Y_{SOU})(t)$ (FISOU) is concerned, by using (4.19) one has:

$$\mathcal{J}^\alpha(Y_{SOU})(t) = \mathcal{J}^\alpha(g_1)(t) + \eta \mathcal{J}^\alpha(g_2)(t), \quad (4.23)$$

with

$$g_1(t) = e^{-\mu t} B(\rho(t)), \quad g_2(t) = e^{-\mu t}, \quad (4.24)$$

where the distributions of the two fractional integrals can be obtained by using Proposition 3.1. By using (4.23), we obtain the covariance of FISOU, for $u \leq t$:

$$\begin{aligned} cov(\mathcal{J}^\alpha(Y_{SOU})(u), \mathcal{J}^\alpha(Y_{SOU})(t)) &= E [\mathcal{J}^\alpha(e^{-\mu u} B(\rho(u))) \mathcal{J}^\alpha(e^{-\mu t} B(\rho(t)))] + \\ &E [\mathcal{J}^\alpha(e^{-\mu u} B(\rho(u))) \eta \mathcal{J}^\alpha(e^{-\mu t})] + E [\eta \mathcal{J}^\alpha(e^{-\mu u}) \mathcal{J}^\alpha(e^{-\mu t} B(\rho(t)))] + \\ &E [\eta \mathcal{J}^\alpha(e^{-\mu u}) \eta \mathcal{J}^\alpha(e^{-\mu t})] := \tilde{J}_1 + \tilde{J}_2 + \tilde{J}_3 + \tilde{J}_4, \end{aligned} \quad (4.25)$$

where for simplicity we let drop the dependence of \tilde{J}_i on α . By using the definition of fractional integral, and proceeding as in the case of FIBM and FIOU, one gets:

$$\tilde{J}_1 = \frac{\tilde{J}_{11} + \tilde{J}_{12} + \tilde{J}_{13}}{\Gamma^2(\alpha)},$$

where:

$$\begin{aligned} \tilde{J}_{11} &= \frac{\sigma^2}{2\mu} \int_0^u ds (u-s)^{\alpha-1} e^{-\mu s} \int_0^s dv (t-v)^{\alpha-1} e^{-\mu v} (e^{2\mu v} - 1) = \tilde{I}_1, \\ \tilde{J}_{12} &= \frac{\sigma^2}{2\mu} \int_0^u ds (u-s)^{\alpha-1} e^{-\mu s} (e^{2\mu s} - 1) \int_s^u dv (t-v)^{\alpha-1} e^{-\mu v} = \tilde{I}_2, \\ \tilde{J}_{13} &= \frac{\sigma^2}{2\mu} \left(\int_0^u ds (u-s)^{\alpha-1} e^{-\mu s} (e^{2\mu s} - 1) \right) \left(\int_u^t dv (t-v)^{\alpha-1} e^{-\mu v} \right) = \tilde{I}_3, \end{aligned}$$

being \tilde{I}_i the integrals concerning FIOU, given by (4.13). Also:

$$\begin{aligned} \tilde{J}_2 &= \frac{\sigma^2}{2\mu} \left(\int_0^u ds (u-s)^{\alpha-1} e^{-\mu s} \cdot \min\{1, e^{2\mu s} - 1\} \right) \left(\int_0^t dv (t-v)^{\alpha-1} e^{-\mu v} \right), \\ \tilde{J}_3 &= \tilde{J}_2, \end{aligned}$$

$$\tilde{J}_4 = \frac{\sigma^2}{2\mu} \left(\int_0^u ds (u-s)^{\alpha-1} e^{-\mu s} \right) \left(\int_0^t dv (t-v)^{\alpha-1} e^{-\mu v} \right).$$

Finally, substituting in (4.25), we obtain for $u \leq t$ the covariance of FISOU:

$$\begin{aligned} \text{cov}(\mathcal{J}^\alpha(Y_{SOU})(u), \mathcal{J}^\alpha(Y_{SOU})(t)) &= \frac{1}{\Gamma^2(\alpha)} \left(\tilde{J}_{11} + \tilde{J}_{12} + \tilde{J}_{13} + 2\tilde{J}_2 + \tilde{J}_4 \right) \\ &= \frac{1}{\Gamma^2(\alpha)} \left(\tilde{I}_1 + \tilde{I}_2 + \tilde{I}_3 + 2\tilde{J}_2 + \tilde{J}_4 \right) = \text{cov}(\mathcal{J}^\alpha(Y_{OU})(u), \mathcal{J}^\alpha(Y_{OU})(t)) + \frac{2\tilde{J}_2 + \tilde{J}_4}{\Gamma^2(\alpha)}. \end{aligned} \quad (4.26)$$

Thus, the covariance function of FISOU turns out to be the sum of the covariance of FIOU and the quantity $\frac{2\tilde{J}_2 + \tilde{J}_4}{\Gamma^2(\alpha)}$.

For $u = t$, one has $\tilde{J}_{13} = 0$ and $\tilde{J}_{11} = \tilde{J}_{12}$, so:

$$\text{var}(\mathcal{J}^\alpha(Y_{SOU})(t)) = \frac{1}{\Gamma^2(\alpha)} \left(2\tilde{J}_{11} + 2\tilde{J}_2 + \tilde{J}_4 \right) = \frac{1}{\Gamma^2(\alpha)} \left(2\tilde{I}_1 + 2\tilde{J}_2 + \tilde{J}_4 \right), \quad (4.27)$$

where all the integrals have to be calculated for $u = t$.

In the Figures 8-9, we report the shape of the variance and covariance function of FISOU, for various values of $\alpha \in (0, 1)$. In the Figure 8, it is observed a time zone (from $t \simeq 1.7$ to $t \simeq 1.8$), at which there is an inversion of behavior, as in Figure 6 concerning the variance of FIOU. Here, however, unlike Figure 6, it is visible a more confused behavior in the time zone (1.7, 1.8). This is probably due to an higher degree of stochasticity of FISOU with respect to FIOU (in fact, the starting point of SOU is random). Note that we have not been able to calculate the variance and covariance of FISOU for α less than 0.1, owing to numerical problems which arise in computing the integrals \tilde{J} , for α near zero. For $\alpha = 0.1$ the curve is close to the graph of the function $v(t) = \sigma^2/2\mu$ (i.e. the variance of SOU), since FISOU for $\alpha = 0$ becomes SOU; for $\alpha \approx 1$ the curve matches the graph of the function $v(t) = \frac{\sigma^2}{\mu^3}(\mu t + e^{-\mu t} - 1)$ (i.e. the variance of ISOU), given by (4.22), since FISOU becomes the ordinary integral of SOU.

5 Some graphical comparisons and concluding remarks

In order to complete our analysis and compare the obtained results for the considered processes, we provide the numerical evaluations of the covariance functions in some three and two dimensional plots.

In the Figure10 we report the two-dimensional color plot of the covariance function of FIBM, $c(u, t) = \text{cov}(\mathcal{J}^\alpha(B)(u), \mathcal{J}^\alpha(B)(t))$, given by (2.8) and the graph of the surface $z = c(u, t)$, for various values of α ; in the Figure 11 we report the graphs of the surface $z = c(u, t)$, for various values of α , in the cases of FIOU and FISOU, respectively. In the Figure 12, we report the two-dimensional color plots of the covariance function of FIOU and FISOU, respectively, for various values of α . These figures illustrate globally the behavior of the covariance function of the three considered processes, for any u and t ; note, for instance, that for $u = t$ they match the behavior shown in the figures concerning the variance of the processes (compare with Figures 6,8).

Comparing the FIOU and FISOU cases of Figg.11-12, the covariances exhibit a similar behavior for values of α greater than 0.8. Furthermore, it appears evidente that the FIOU and FISOU covariances are always lower than those of FIBM in Fig. 10. The behaviors

of FIOU and FISOU covariance appear more similar each other, but really different from the behavior of the FIBM covariance. Indeed, in Fig.10 is evident that the covariance of FIBM, as function of α , and for increasing α , attains rapidly values around 15, whereas the covariances of FIOU and FISOU arrive to around 2, for $\alpha \approx 1$.

Moreover, referring to color plot of the covariances of FIOU and FISOU in Fig.12, we note that for every values of α the FISOU covariance, although slightly, has values greater than those of the FIOU covariance. In addition, the FISOU covariance show higher values (consequently, it can be seen a more diffuse correlation) around the diagonal respect to the case of FIOU covariance. In particular, note that, for $\alpha = 0.2$ in Fig.12, FISOU covariance $c(u, t)$ shows highest values for small values of t and u close to the diagonal, differently from the FIOU covariance. For $\alpha = 0.5$ and $\alpha = 0.8$ the color plots of FISOU become more similar to those of FIOU, even if a more diffusion correlation remains evident for FISOU case. An explanation of these differences can be that the SOU process has a random starting point, and this has an impact on the ISOU, implying a greater variability (larger variance and correlation) respect to the case of IOU process.

The above comparing remarks can also be verified in the three-dimensional plots in Fig.11, where it is also possible to observe how the covariance functions increase for increasing values of α .

However, for large enough time t , variance and covariance of the three processes are increasing functions of α , as one expects.

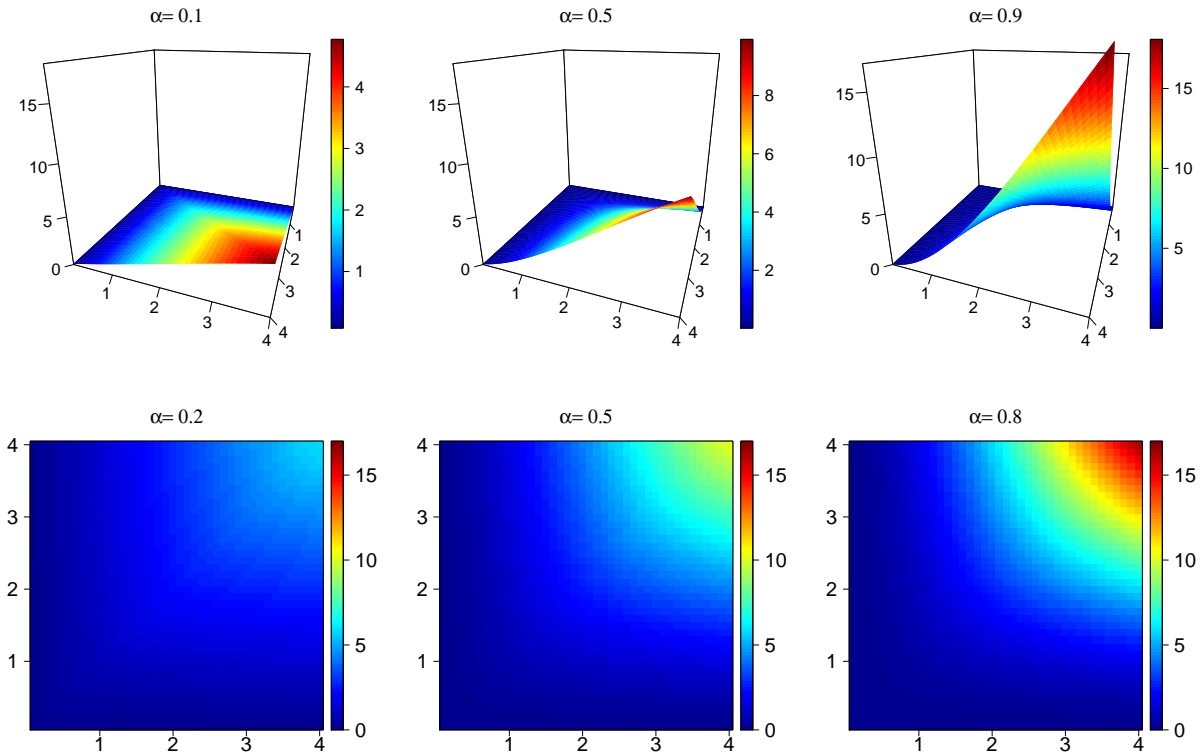


Figure 10: On top: three-dimensional plot of the covariance function of FIBM $cov(\mathcal{J}^\alpha(B)(u), \mathcal{J}^\alpha(B)(t))$, for $\sigma = \mu = 1$, and various values of α . On bottom: two-dimensional color plot of the covariance function of FIBM $cov(\mathcal{J}^\alpha(B)(u), \mathcal{J}^\alpha(B)(t))$ on the same scale.

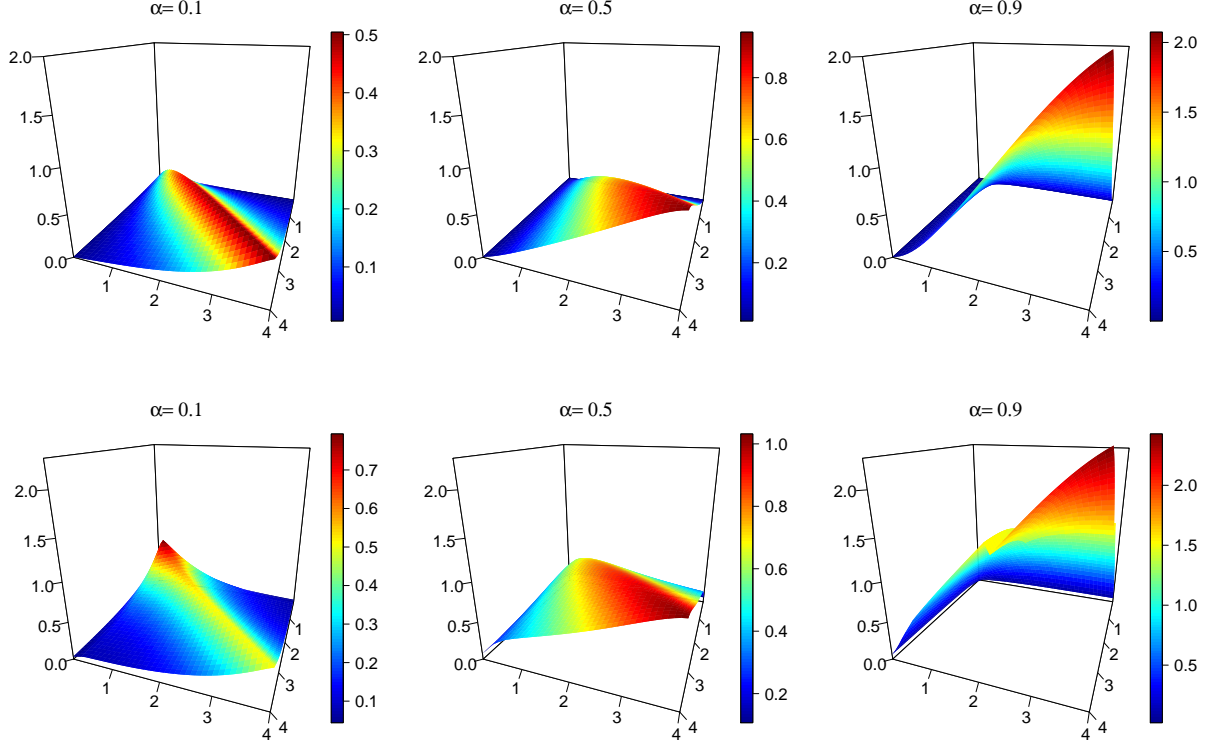


Figure 11: On top: three-dimensional plot of the covariance function of FIOU $c(u, t) = cov(\mathcal{J}^\alpha(Y_{OU})(u), \mathcal{J}^\alpha(Y_{OU})(t))$ for $\sigma = \mu = 1$, and various values of α . On bottom: the same for the covariance function of FISOU $c(u, t) = cov(\mathcal{J}^\alpha(Y_{SOU})(u), \mathcal{J}^\alpha(Y_{SOU})(t))$.

We remark the usefulness of the graphical comparisons for the considered processes and for different values of fractional order α . Again we confirm that the parameter α can be extremely useful in models, similar to the proposed neuronal model, for tuning the length of memory and the accuracy of the time-scale of dynamics under observation.

The aim of giving further contribution to neuronal modeling led us to consider the long range memory process obtained as the fractional integral over time of a GM process. In particular, the adoption of the fractional integral operator in place of the integer one, extending (from mathematical point of view) the latter, allows to describe dynamics that occur on different time-scales on which the integration of their past evolution plays the key rule to understand and predict the resultant complex behaviors.

In this paper, motivated by the above considerations, we have studied as replacing the ordinary Riemann integral with the fractional RL integral of order $\alpha \in (0, 1)$ affects the behavior, when varying α , of an integrated GM process, i.e. the processes obtained applying the fractional RL integral over time to GM processes; in particular, we have studied the fractional integral of Brownian motion, non-stationary OU process and stationary OU process. These processes have a preminent use in neuronal modeling and they are representative of the main classes of GM processes. Beyond the closed-form obtained of covariance function of each of the above processes, we also provide numerical and graphical results, suitably compared. The possible applications by means of a neuronal model are illustrated. The advantage of the evaluations of covariances for fractional integrated processes is in the possibility to implement a simulation procedure for sample paths and the consequent investigation

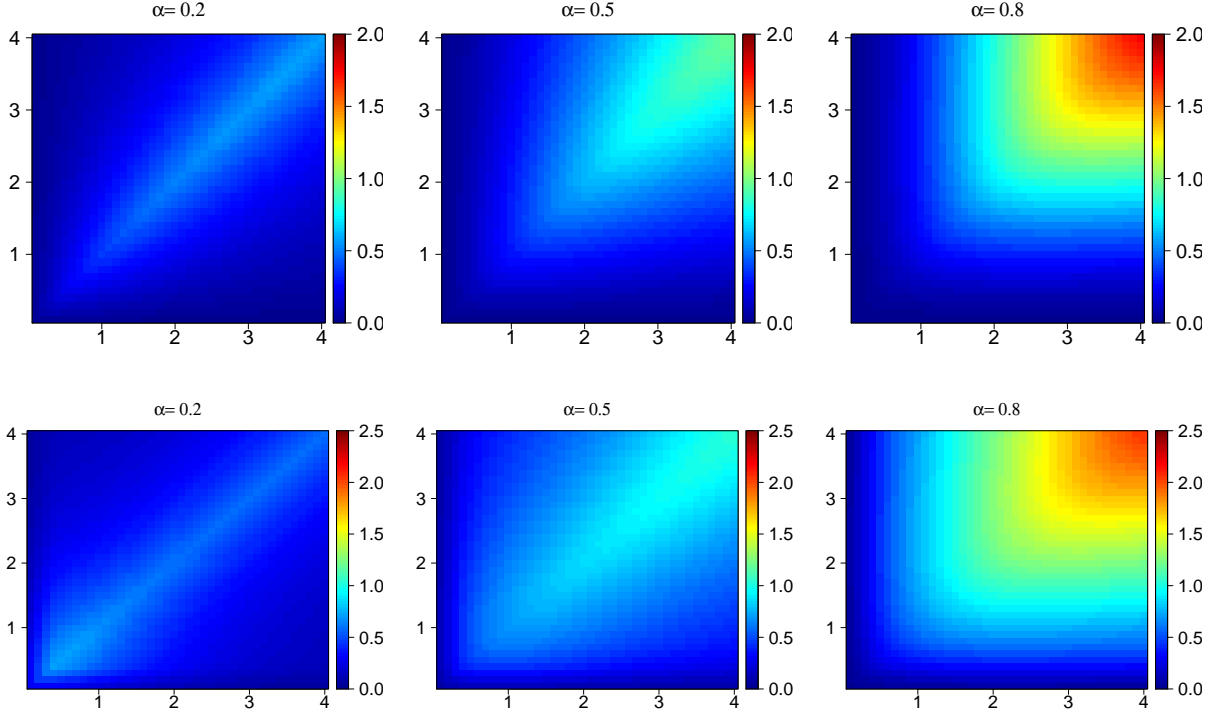


Figure 12: On top: two-dimensional color plot of the covariance function of FIOU $c(u, t) = cov(\mathcal{J}^\alpha(Y_{OU})(u), \mathcal{J}^\alpha(Y_{OU})(t))$, for $\sigma = \mu = 1$, (on the same scale) and various values of α . On bottom: the same for the covariance function of FISOU $c(u, t) = cov(\mathcal{J}^\alpha(Y_{SOU})(u), \mathcal{J}^\alpha(Y_{SOU})(t))$.

of the first passage times through specific boundaries ([3],[40]). This will be of extreme interest to explain and predict neuronal dynamics, because none theoretical result about these times for fractional integrated processes is available. All these further investigations will be the object of our future work.

References

- [1] Abundo, M., 2015. On the first-passage time of an integrated Gauss-Markov process. *Scientiae Mathematicae Japonicae Online e-2015*, 28, 1–14.
- [2] Abundo, M., 2013. On the representation of an integrated Gauss-Markov process. *Scientiae Mathematicae Japonicae Online e-2013*, 719–723.
- [3] Abundo, M., 2017. The mean of the running maximum of an integrated GaussMarkov process and the connection with its first-passage time . *Stochastic Analysis and Applications*. Volume 35, Issue 3, Pages 499-510
- [4] Abundo, M., Pirozzi, E., 2017. Integrated stationary OrnsteinUhlenbeck Process, and double integral processes. *Physica A*, <https://doi.org/10.1016/j.physa.2017.12.043>
- [5] Abundo, M., 2012. An inverse first-passage problem for one-dimensional diffusions with random starting point. *Statistics and Probability Letters* 82 (1), 7–14.

- [6] Ascione, G., Pirozzi, E. 2018. On Fractional Stochastic Modeling of Neuronal Activity Including Memory Effects. LNCS, volume 10672, pp 3-11.
- [7] Ascione, G., Leonenko, N. Pirozzi, E. 2018. Fractional Queues with Catastrophes and Their Transient Behaviour. *Mathematics*, 6, 159; doi:10.3390/math6090159
- [8] Ascione, G., Pirozzi, E. 2019. On a stochastic neuronal model integrating correlated inputs. Submitted.
- [9] Baleanu, D. , Diethelm, K., Scalas, E., Trujillo, J. 2009. *Fractional Calculus Models and Numerical Methods*, World Scientific, Singapore.
- [10] Barndorff-Nielsen, O.E., Shephard, N., 2003. Integrated OU Processes and Non-Gaussian OU-based Stochastic Volatility Models. *Scandinavian Journal of Statistics* 30, 277–295.
- [11] Bazzani, A., Bassi, G., Turchetti, G., 2003. Diffusion and memory effects for stochastic processes and fractional Langevin equations. *Physica A* 324, 530–550.
- [12] Burkitt, A. N., 2006. A review of the integrate-and-fire neuron model: I. Homogeneous synaptic input, *Biological Cybernetics*, 95 , 119.
- [13] Caputo, M., 1967. Linear models of dissipation whose Q is almost frequency independent–II. *The Geophysical Journal of the Royal Astronomical Society* 13, 529–539.
- [14] Cui, Z. and Nguyen, D., First Hitting Time of Integral Diffusions and Applications. 2017. *Stochastic Models* Volume 33, Issue 3, Pages 376-391.
- [15] Debnath, L., 2003. Fractional integral and fractional differential equations in fluid mechanics. *Fractional Calculus and Applied Analysis* 6(2), 119–155.
- [16] Ferreira, A., de Haanb, L., Zhou, C., 2012. Exceedance probability of the integral of a stochastic process. *Journal of Multivariate Analysis*, Volume 105, Issue 1, Pages 241-257.
- [17] Haugh M., *Generating Random Variables and Stochastic Processes*, IEOR E4703: Monte Carlo Simulation, Columbia University
- [18] Hilfer, R. , 2000. *Applications of Fractional Calculus in Physics*, World Scientific, River Edge, NJ, USA
- [19] Ishteva, M.K., 2005. Properties and Applications of the Caputo Fractional Operator. Master Thesis. Department of Mathematics, Universitat Karlsruhe, Sofia (Bulgaria). http://homepages.vub.ac.be/~mishteva/papers/Ishteva_MScThesis.pdf
- [20] Jafarpour, E., Michael Vennettilli, M. and Iyer-Biswas, S. 2017 Biological timekeeping in the presence of stochasticity. <https://arxiv.org/pdf/1703.10058.pdf>
- [21] Kilbas, A.A., Srivastava, H.M., Trujillo, J.J. 2006. *Theory and applications of fractional differential equations*, vol 204. North-Holland mathematics studies. Elsevier, Amsterdam

- [22] Kim, H., Shinomoto, S., 2014. Estimating nonstationary inputs from a single spike train based on a neuron model with adaptation *Math. Bios. Eng.* 11, 49-62.
- [23] Kobayashi, R., Tsubo, Y., Shinomoto, S., 2009. Made-to-order spiking neuron model equipped with a multi-timescale adaptive threshold. *Frontiers in Computational Neuroscience* 3-9.
- [24] Kroese, D.P., Taimre, T., Botev, Z.I., 2011. *Handbook of Monte Carlo Methods*. Wiley Series in Probability and Statistics, John Wiley & Sons, Hoboken, NJ.
- [25] Lakshmikantham, I., Leela, S., 2009. *Theory of Fractional Dynamical Systems*, Cambridge Scientific Publishers, Cambridge, UK
- [26] Lansky, P., Ditlevsen, S.. 2008. A review of the methods for signal estimation in stochastic diffusionleaky integrate-and-fire neuronal models. *Biol Cybern* 99:253262 DOI 10.1007/s00422-008-0237-x
- [27] Li, C., Qian, D., Chen, Y. 2011. On Riemann-Liouville and Caputo Derivatives. *Discrete Dynamics in Nature and Society* Volume 2011, Article ID 562494, doi:10.1155/2011/562494
- [28] Lim S.C., Eab, C. H., Some fractional and multifractional Gaussian processes: A brief introduction. *International Journal of Modern Physics: Conference Series* Vol. 36, 1560001
- [29] Malinowska, A.B. et al. 2015. *Advanced Methods in the Fractional Calculus of Variations*, Springer Briefs in Applied Sciences and Technology, DOI 10.1007/978-3-319-14756-7_2
- [30] Meerschaert, M. M., Sabzikar, F. 2014. Stochastic Integration For Tempered Fractional Brownian Motion. *Stochastic processes and their applications*, 124(7), 2363-2387.
- [31] Nobile, A.G., Pirozzi, E., Ricciardi, L.M., 2008. Asymptotics and evaluations of FPT densities through varying boundaries for Gauss-Markov processes. *Scientiae Mathematicae Japonicae* 67, (2), 241-266.
- [32] Pirozzi, E., 2017. Colored noise and a stochastic fractional model for correlated inputs and adaptation in neuronal firing. *Biol Cybern* 1-15, <https://doi.org/10.1007/s00422-017-0731-0>
- [33] Podlubny, I. 1999. *Fractional differential equations*. Academic Press, San Diego
- [34] Revuz, D. and Yor, M., 1991. *Continuous martingales and Brownian motion*. Springer-Verlag, Berlin Heidelberg.
- [35] Ross, S.M., 2010. *Introduction to Probability Models*. Tenth Edition. Academic Press, Elsevier, Burlington
- [36] Samko, S. G. , Kilbas, A. A., Marichev, O. I. 1993. *Fractional Integrals and Derivatives: theory and applications*, Gordon and Breach Science Publishers, Switzerland

- [37] Sakai, Y., Funahashi, S., Shinomoto, S. 1999. Temporally correlated inputs to leaky integrate-and-fire models can reproduce spiking statistics of cortical neurons. *Neural Netw* 12:1181-1190
- [38] Sithi, V.M., Lim S.C. 1995. On the spectra of Riemann-Liouville fractional Brownian motion, *Journal of Physics A: Mathematical and General*, 29:2995-3003.
- [39] Stein, M.L., 1995. Predicting Integrals of Stochastic Processes *Ann. Appl. Probab.*, Volume 5, Number 1, 158-170.
- [40] Taillefumier, T., Magnasco, M.O., 2010. A Fast Algorithm for the First-Passage Times of Gauss-Markov Processes with Holder Continuous Boundaries. *Journal of Statistical Physics* 140(6), 1130–1156.
- [41] Taylor, J.M.G., Cumberland, W.G., and Sy, J.P., 1994. A Stochastic Model for Analysis of longitudinal AIDS Data. *J. Amer. Statist. Assoc.* 89, No. 427, Applications & Case Studies, 727–736.
- [42] Tamura, S., Nishitani Y., Hosokawa C., Mizuno-Matsumoto Y. 2018. Asynchronous Multiplex Communication Channels in 2-D Neural Network With Fluctuating Characteristics, in *IEEE Transactions on Neural Networks and Learning Systems*. doi: 10.1109/TNNLS.2018.2880565
- [43] Teka, W., Marinov, T.M., Santamaria, F. 2014. Neuronal spike timing adaptation described with a fractional leaky integrate-and-fire model. *PLoS Comput Biol* 10:e1003526
- [44] Touboul, J. and Faugeras, O., 2008. Characterization of the first hitting time of a double integral processes to curved boundaries. *Adv. Appl. Prob.* 40, 501–528.